Macromolecular Chemistry and Physics
www.mcp-journal.de

RAFT Synthesis of Reactive Multifunctional Triblock-Copolymers for Polyplex Formation

*Nicolas Ritt, Amal Ayaou, and Rudolf Zentel**

Reversible addition–fragmentation chain transfer polymerization with a low-temperature initiator can be used to synthesize multifunctional block copolymers for polyplex formation. Utilizing three methacrylate monomers (triethylene glycol methyl ether methacrylate (MEO_3MA), pyridyldisulfideethyl methacrylate (PDSM), *N*,*N*-dimethylethylenediamine methacrylate (DMAEMA)) and an azide bearing chain transfer agent for polymerization, the resulting triblock-copolymers possess two orthogonally reactive functionalities (a block with reactive disulfide side chains and an azide end-group) and two additional functional blocks for i) solubilization and ii) polyplex formation. Thereby, the MEO_3MA block provides solubility in aqueous media and the DMAEMA block, having a tertiary amine in the side chain, allows polyplex formation with polyanionic biomacromolecules like DNA or RNA. Due to the reactive disulfide block the polyplexes can be (reversibly) crosslinked with dithiols. Because of the manifold of possibilities to modify the pDNApolyplexes, this polymers system is an interesting candidate for active-targeting and codelivery approaches.

1. Introduction

Over the last decades nanoformulated drug delivery systems, also termed nanomedicines, have become a focus of interest for various fields of clinical research. Especially for the treatment of inherited or acquired genetic diseases, the use of nonviral agents for gene therapy has been a widely discussed matter.[1–6] Concerning tumor therapy, Doxil, Abraxane, Narekt-102, Paclical, and other therapeutics are well known examples.[7–9]

In general, nanoformulated drug delivery systems can provide several advantages. For example, poorly soluble drugs can be solubilized and thereby harnessed for therapy. Additionally, early blood clearance and degradation can be reduced, which leads to prolonged blood circulation times.[10,11] Especially for the utilization of DNA or various types of RNA, nanomedical formulations are essential, because intravenous administration of naked DNA or RNA leads to fast degradation by nucleases[12] and an unspecific activation of the immune system. In addition to that, nucleic acids cannot traverse the cellular membrane by diffusion, due to their size and polyanionic nature. Hence, transport systems for nucleic acids need to provide a protective shell that is able to mask the payload and its anionic charge from the physiological medium, ensures cellular uptake and intracellular release. In this respect, polyplexes, which are formed by electrostatic interaction of cationic polymer components and the negatively charged backbone of the nucleic acid, pose an elegant solution. The electrostatic interaction masks the polyanionic properties of the nucleic acid, thereby promoting cellular uptake and reducing interaction with plasma proteins. The perfect transport systems for nucleic acids shall thus consist of an internal core to stabilize the polyanionic nucleic acid and a well water-soluble, stealth-like shell to shield the core from interactions with nucleases and generally prevent extensive unspecific interactions with proteins.[13] In addition to that, functional groups, which can be addressed in an aqueous environment to allow reversible stabilization of the polyplex, and the addition of targeting groups like antibodies, certain protein- or carbohydrate structures onto the particle's surface are desirable. This can help to promote an accumulation of the nanomedical agent in the target tissue and lead to a higher rate of drug internalization. Because of this, a functional interlayer between the charged core and the stealth-like corona is attractive.

For systemically application of a polymer-based drug delivery system, it is also important to differentiate between the transport form of a nanomedical therapeutic and its delivery form. Between the administration of a drug and reaching the target cell, the nanomedicine must have a high stability and a high half-life time. However, after the drug is taken up by the target cell, an efficient release of the payload must follow. The change in stability of the transport system must result from to a certain intracellular stimulus This could for example be a response to the decreasing pH levels upon endosomal uptake,[14,15] or a response to the change in the redox potential upon entering the cytosol.[16–20] In this respect, a reversible disulfide crosslinking

N. Ritt, A. Ayaou, Prof. R. Zentel
Department of Chemistry
Johannes Gutenberg University Mainz
Duesbergweg 10–14, 55128 Mainz, Germany
E-mail: zentel@uni-mainz.de

The ORCID identification number(s) for the author(s) of this article can be found under https://doi.org/10.1002/macp.202100122

© 2021 The Authors. Macromolecular Chemistry and Physics published by Wiley-VCH GmbH. This is an open access article under the terms of the Creative Commons Attribution-NonCommercial License, which permits use, distribution and reproduction in any medium, provided the original work is properly cited and is not used for commercial purposes.

DOI: 10.1002/macp.202100122

Check for updates
15213935, 2021, 16, Downloaded from https://onlinelibrary.wiley.com/doi/10.1002/macp.202100122 by Cochrane Germany, Wiley Online Library on [17/10/2022]. See the Terms and Conditions (https://onlinelibrary.wiley.com/terms-and-conditions) on Wiley Online Library for rules of use; OA articles are governed by the applicable Creative Commons License

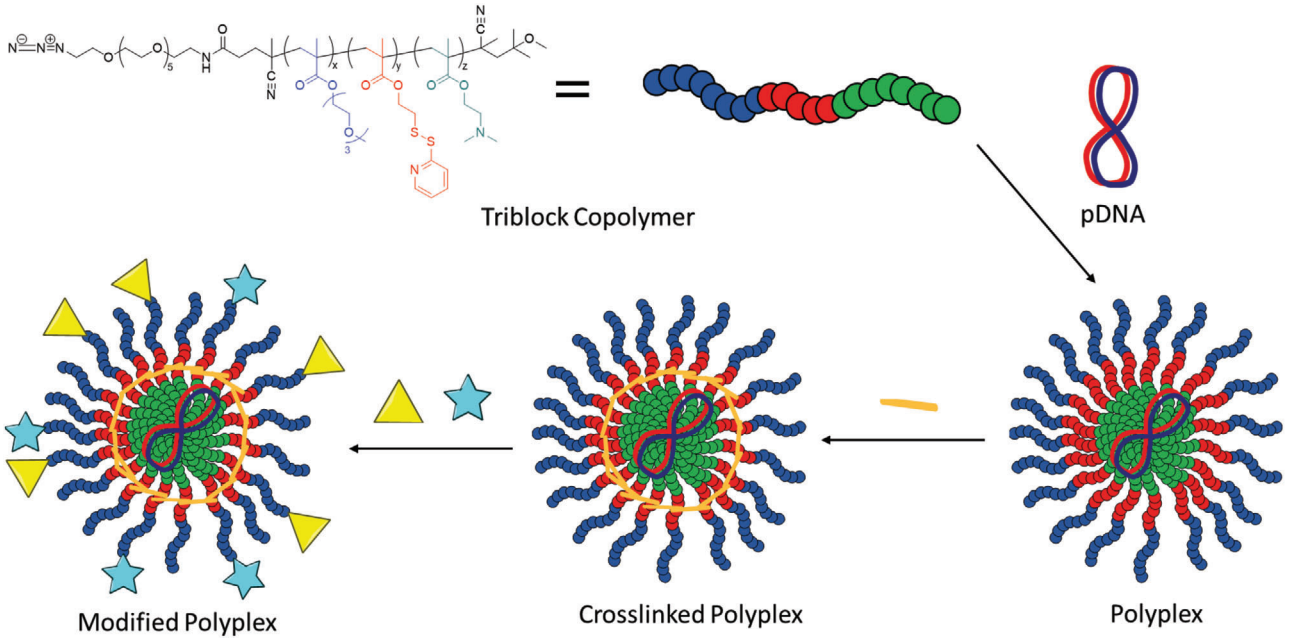

Figure 1. Rational of polyplex synthesis and modification.

of nanomedical formulations is particularly interesting, as disulfide bonds are fairly stable during blood circulation and in the extracellular medium, but can easily be cleaved by glutathione (GHS) in the cytosol. In addition, targeting functions can be a factor to increase the delivery efficiency.

Polymer chemistry provides us with various techniques to prepare statistical and multiblock polymers and a multitude of possible building blocks to construct elaborate polymers for polyplex formation. Up until now, several statistical polymers, simple block- and graft-copolymers and combinations of statistical and block-copolymers have been synthesized for DNA complexation and delivery. As cationic components for polyplex formation, poly(ethylene imine), poly(*N*,*N*-dimethylaminoethyl) structures, poly(L-lysine) and several other structures that bear primary, secondary, tertiary or quarternized amines have been used frequently.[21–30] Incorporation of poly(ethylene glycol), poly(2-oxazoline), or polysarcosine increases the solubility of the polyplex and further decreases interaction with blood components.[12,31–39]

Up until now, various delivery systems and polymer architectures have been synthesized and tested for their applicability for polyplex formation and gene delivery.[34,40–43] Barz and co-workers could show that an arrangement of the functional monomer units into three different polymer blocks, thus spatially separating different functional units from one another in the final polyplex (see **Figure 1**), leads to improved polyplex stability and transfection when compared to polyplexes formed from random polymer structures.[44] The polypept(o)id prepared for this purpose consisted of a cationic block, an intermediate block with reactive disulfide units (reversible crosslinking) and a stealth-like polysarcosine block. Thus, with regard to poly-methacylates as alternative polymer structures, multifunctional block-copolymers as presented in Figure 1, are interesting. Recently such triblock-copoly-methacrylates were prepared for the first time, but their synthesis required several post-polymerization reactions.[45] Here we describe the direct synthesis of such multifunctional block-copolymers by reversible addition–fragmentation chain transfer (RAFT) polymerization. Additionally, they are functionalized with an azide end group for strain-promoted azide-alkyne cycloaddition (SPAAC).

2. Results and Discussion

2.1. Polymer Synthesis

We wanted to develop a synthetic route to a triblock-copolymer system for the formation of polyplexes with plasmid DNA vectors, which can be functionalized further in a stimulus-responsive way (see Figure 1). First of all, this block-copolymer should combine a cationic core to complex the polyanionic DNA (or RNA) with a rather stealth-like polymer corona to minimize unspecific interactions with plasma proteins. Such structures are often used for polyplex formation.[32,35,38,39,46] But in addition to that, it should contain an additional reactive, intermediate block for a further stimulus responsive functionalization in aqueous media (see Figure 1). This may include the addition of further bioactive compounds or a reversible stabilization of the polyplex by crosslinking (transport form). For this purpose, reactive disulfides are attractive. They react quickly with soft nucleophiles but are rather unreactive to the hard nucleophile hydroxide anion in water. Furthermore, after cellular uptake, they are easily cleaved in the cytosol due to an increased concentration of GHS. For further functionalization we used an azide group in the chain transfer agent (CTA) to allow the addition of possible targeting units to the water-soluble polymer corona.

Thus, to prepare the multifunctional triblock-copolymers according to Figure 1, three different monomers were utilized in a sequential RAFT polymerization process (see **Figure 2**).

© 2021 The Authors. Macromolecular Chemistry and Physics published by Wiley-VCH GmbH

15213935, 2021, 16, Downloaded from https://onlinelibrary.wiley.com/doi/10.1002/macp.202100122 by Cochrane Germany, Wiley Online Library on [17/10/2022]. See the Terms and Conditions (https://onlinelibrary.wiley.com/terms-and-conditions) on Wiley Online Library for rules of use; OA articles are governed by the applicable Creative Commons License

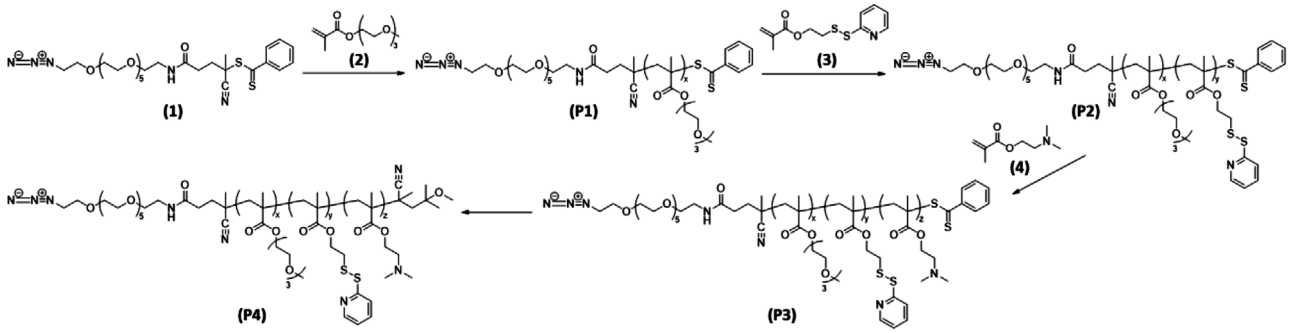

Figure 2. RAFT polymerization steps for block-copolymerization.

In our approach, the hydrophilicity and stealth-like properties are mediated by triethylene glycol methyl ether methacrylate (MEO_3MA; Figure 2(2)) which was already successfully applied in the synthesis of nanosized systems for the encapsulation of mRNA and siRNA.[47,48] As reactive disulfide component pyridyldisulfideethyl methacrylate (PDSM; Figure 2(3)) was used. Reactive disulfides like PDSM have proven to undergo fast and quantitative disulfide-exchange reactions in the synthesis of polypept(o)id structures and other polymers.[45,49–51] The resulting disulfide is prone to reductive degradation, which can be used as stimulus to tune the stability of the polyplex by reversible crosslinking. In addition to that, small molecule drugs could be covalently bound for co-delivery. In the extra- and intracellular environment GHS is the mainly responsible reductive agent for cleaving disulfide bonds in the physiological environment. Typically, the extracellular concentration of GHS is fairly low, with values between 2×10^{-6} and 20×10^{-6} M, whereas the intracellular GHS concentration is between 0.5×10^{-3} and 10×10^{-3} M.[52] Because of this big gradient, cleavage of disulfide bonds is mainly facilitated in the cytosol. The crosslinked polyplexes should thus possess improved stability in the blood stream but get destabilized after the uptake into the cell. This can potentially lead to an improvement of pDNA transport and uptake. In addition to that, SPAAC modification of the azide end group of the polymers and disulfide exchange reaction are orthogonal to one another, as there is no cross-reactivity. Hence, modification can be, in principle, facilitated in a one-pot synthesis. For the polycationic block *N*,*N*-dimethylethylenediamine methacrylate (DMAEMA; Figure 2(4)) was used. As methacrylate, it is well compatible with the two other methacrylate-based monomers. In addition to that, it is biocompatible.[25,38] The tertiary amine-bearing side chain of this component is fully protonated under physiological conditions, offering the opportunity to complex DNA or RNA molecules. Additionally, when the polyplex is taken up into the endosome, the polycationic p(DMAEMA) block shall improve the endosomal escape by interacting and distorting the mainly negatively charged endosomal membrane.

RAFT polymer synthesis was conducted by three consecutive polymerization steps and a fourth step, deactivating the reactive CTA end group (see Figure 2).

As CTA 1-azido-25-cyano-22-oxo-3,6,9,12,15,18-hexaoxa-21-azahexadodecan-25-yl benzothioate (further referred to as azide-CTA) was used. The azide-CTA was synthesized similar to the two-step-reaction published by Nuhn et al.[47] and Kramer et al.[53] The included azide group is connected to a hydrophilic oligo ethylene oxide spacer to improve its presentation in the hydrophilic polymer shell. Thus, it is also possible to click highly polar targeting units to a preformed nanoparticle.[53] To initiate the polymerization reactions, 2,2'-azo-di(4-methoxy-2,4-dimethylvaleronitrile) (AMDVN) was used, which has, in comparison to other initiation agents, a fairly low activation temperature. The half-life of AMDVN at 30 °C is comparable to the half-life of AIBN at 80 °C.[47] Therefore, polymerization reactions could be conducted at ambient temperatures whilst still providing efficient monomer conversions. Additionally, the low reaction temperature is advantageous to prevent azide degradation during polymerization, and it can help to minimize side-reactions of the reactive disulfide in PDSM with the amines in DMAEMA. After each step of the polymerization reaction, the respective polymer product was isolated and purified by several precipitation steps, as described above. The successive polymerization of the triblock-copolymers was accompanied by extensive ^{1}H-NMR measurements to determine monomer conversion and degree of polymerization. In addition to that, size exclusion chromatography (SEC) was used to determine the polydispersity of the respective polymers.

Table 1. Characterization of p(MEO_3MA) homopolymers.

Polymer	DP_x [a]	M_n [b] [g mol^{-1}]	$Đ$ [c]
P1-1	30	7580	1,20
P1-2	40	9900	1,17
P1-3	47	11 530	1,19

[a] Degree of polymerization of the MEO_3MA block; [b] Number-average molecular weight as determined by NMR spectroscopy; [c] Polydispersity as determined by SEC.

The polymerization of MEO_3MA was conducted over the duration of 21–24 h. For the polymer synthesis a target conversion of 60% was aimed for. When the targeted conversion rate was met, the reaction was quenched by exposure of the reaction vessel to liquid nitrogen, and the product was purified by successive precipitation steps. For the polymers featured in this study, degrees of polymerization of 30/40/47 units of MEO_3MA were synthesized, as depicted in **Table 1**. These polymers were highly uniform with a polydispersity of 1.17–1.20. The degree of polymerization could be tuned at will by altering the monomer to CTA ratio.

© 2021 The Authors. Macromolecular Chemistry and Physics published by Wiley-VCH GmbH

15213935, 2021, 16, Downloaded from https://onlinelibrary.wiley.com/doi/10.1002/macp.202100122 by Cochrane Germany, Wiley Online Library on [17/10/2022]. See the Terms and Conditions (https://onlinelibrary.wiley.com/terms-and-conditions) on Wiley Online Library for rules of use; OA articles are governed by the applicable Creative Commons License

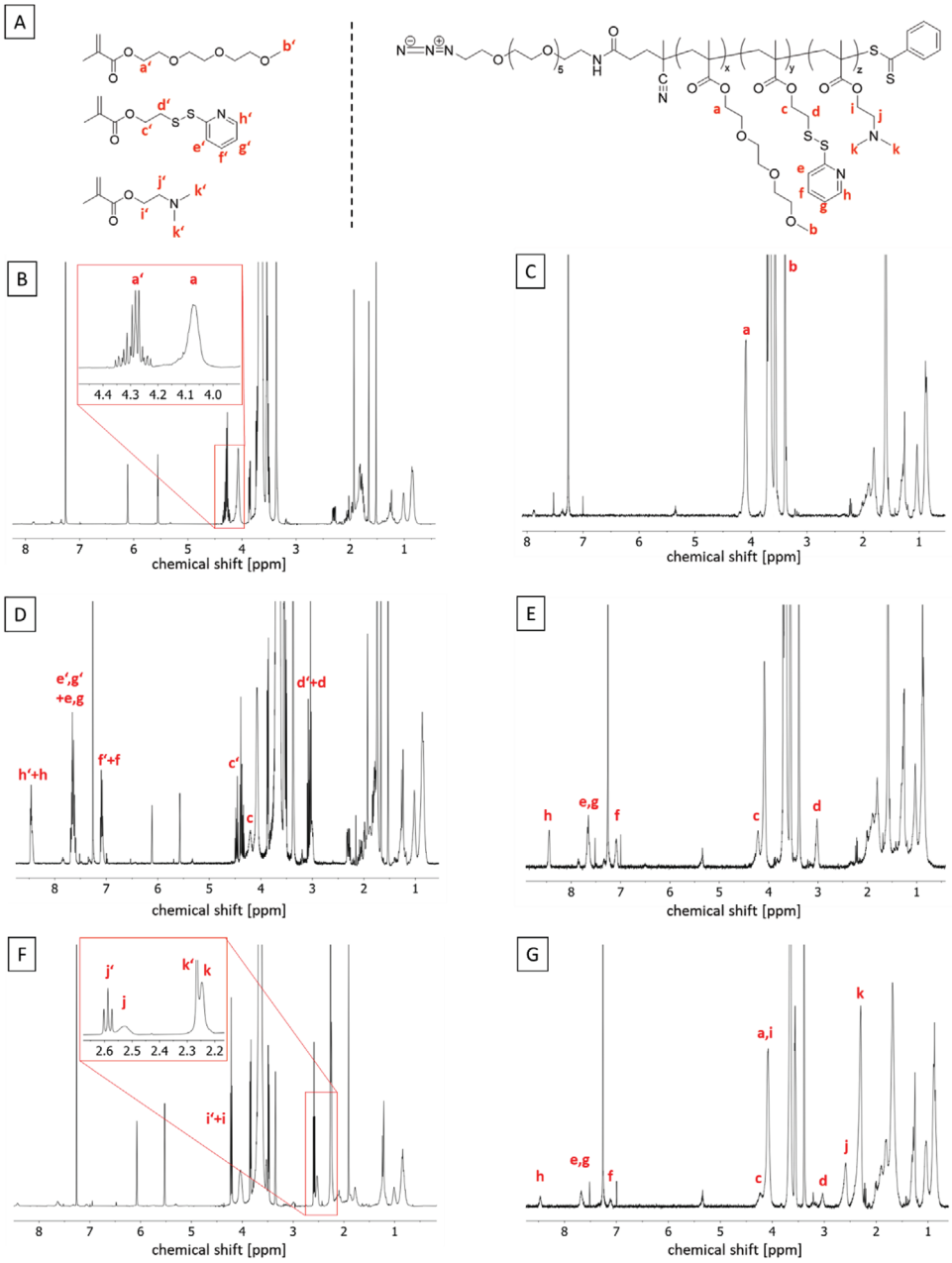

Figure 3. A) Triblock-copolymer and the corresponding monomer species. B) Conversion NMR of P1-4 homopolymerization. C) ^{1}H-NMR of P1-4. D) Conversion NMR of P2-4 diblock-copolymerization. E) ^{1}H-NMR of P2-4. F) Conversion NMR of P3-4 triblock-copolymerization. G) ^{1}H-NMR of P3-4.

Successively, p(MEO_3MA)-*b*-p(PDSM) diblock-copolymers were synthesized. Either 5 or 10 units of PDSM were targeted for to build the second, reactive disulfide polymer block. The polymerization reaction was conducted for 16–19 h over night with a target conversion of about 50%. For the calculation of monomer conversion, after normalization of the methylene proton signals of the methacrylate monomer, the intensities of the overlapping signals of the monomer and polymer side chain protons were compared, and the arithmetical mean was calculated (see **Figure 3**D). The increase of the average molecular weight could be detected by SEC, and integrity of the PDSM reactive side chain group was confirmed by ^{1}H-NMR analysis. In addition to that, diffusion ordered nuclear resonance spectroscopy (DOSY NMR) showed that all signals that can be attributed to MEO_3MA and PDSM repetition units were part of one molecular species. This indicates that no homo-polymerization of PDSM took place and block-copolymerization followed the RAFT mechanism. In addition to that, polydispersities were narrow with values between 1.16 and 1.25 (see **Table 2**).

As third step of block-copolymerization, the synthesized p(MEO_3MA)-*b*-p(PDSM) diblock-copolymers were used as macro-CTA for the polymerization of DMAEMA. For the

© 2021 The Authors. Macromolecular Chemistry and Physics published by Wiley-VCH GmbH

15213935, 2021, 16, Downloaded from https://onlinelibrary.wiley.com/doi/10.1002/macp.202100122 by Cochrane Germany, Wiley Online Library on [17/10/2022]. See the Terms and Conditions (https://onlinelibrary.wiley.com/terms-and-conditions) on Wiley Online Library for rules of use; OA articles are governed by the applicable Creative Commons License

Table 2. Characterization of p(MEO_3MA)-*b*-p(PDSM) diblock-copolymers.

Polymer	DP_x [a]	DP_y [b]	M_n [c] [g mol^{-1}]	$Đ$ [d]
P2-1	30	4	8600	1.18
P2-2	40	4	10 925	1.19
P2-3	47	10	14 080	1.18

[a] Degree of polymerization of the MEO_3MA block; [b] Degree of polymerization of the PDSM block; [c] Number-average molecular weight as determined by NMR spectroscopy; [d] Polydispersity as determined by SEC.

Table 3. Characterization of p(MEO_3MA)-*b*-p(PDSM)-p(DMAEMA) triblock-copolymers.

Polymer	DP_x [a]	DP_y [b]	DP_z [c]	M_n [d] [g mol^{-1}]	$Đ$ [e]
P3-1	30	4	25	12 530	1.24
P3-2	40	4	11	12 650	1.25
P3-3	47	10	16	16 600	1.19
P3-4	47	10	47	21 470	1.16

[a] Degree of polymerization of the MEO_3MA block; [b] Degree of polymerization of the PDSM block; [c] Degree of polymerization of the DMAEMA block; [d] Number-average molecular weight as determined by NMR spectroscopy; [e] Polydispersity as determined by SEC.

triblock-copolymers, a percental share of the hydrophilic p(MEO_3MA) block of either 75%, 66% or 50% was intended. The ratios of macro-CTA to monomer were adjusted to meet the intended degree of polymerization at a conversion rate of 50%. Reactions were conducted for 22–44 h. As the targeted conversion was confirmed by ^{1}H-NMR spectroscopy (see Figure 3F), the reaction was quenched as described. DOSY NMR spectroscopy (see **Figure** 4A) showed that the signals belonging to the DMAEMA side chains and the signals that are caused by the side chains of the diblock-copolymer can be attributed to a single molecular species. This confirms that the polymerization of the third polymer block followed the RAFT polymerization mechanism, and no homo-polymerization of DMAEMA took place. SEC data (see Figure 4B) could be misinterpreted, as it indicates a decline in molecular weight when comparing the diblock-copolymer (b) and triblock-copolymer (c) SEC curves. This can be explained with the change in hydrophilic properties, caused by the slightly hydrophobic DMAEMA repetition units, leading to a contraction of the polymer coil and thus a decrease in the hydrodynamic diameter of the polymers. However, polydispersities as determined by SEC were very narrow, ranging from 1.16 to 1.25 (see **Table 3**).

For each individual step of the RAFT polymerization process, it was possible to tune individual block lengths at will by tuning the (macro-) CTA to monomer ratio. The synthesis gave highly reliable and reproduceable results with overall narrow molecular weight distributions. In addition to that, the integrity of the azide end group was monitored after each polymerization step by infrared (IR) spectroscopy. Because of the decreasing percental contribution of the azide end group to the molecular composition of the polymer, the intensity of the azide signal in the IR spectra decreased from polymerization step to polymerization step. However, a reasonable azide signal could still be detected in the triblock-copolymer even after deactivation of the reactive RAFT end group (see paragraph below and **Figure 5**). Because of its low concentration in the triblock-polymer it was, however not possible to quantify the amount of azide groups.

To prevent uncontrolled reactions at the reactive benzothioate end group of the triblock-coplymers, a fourth reaction step was applied to deactivate it. Hence, the triblock-copolymers were reacted with a large molar excess of AMDVN (first with 30, later with 15 equivalents) to remove the benzothioate end group. The reaction was monitored using ultraviolet-visible (UV–Vis) spectroscopy. Over the cause of 24 to 48 h the absorption maximum of the benzothioate group at a wavelength of about 410 nm disappeared. This could also be precepted by the gradual fading of the light red color, caused by the loss of the RAFT end group. In addition to that, no traces of the benzothioate group could be detected by ^{1}H-NMR spectroscopy. However, for polymer batches treated with large amounts of AMDVN (30 equivalents), ^{1}H-NMR spectroscopy indicated partial cleavage of reactive PDSM groups. This can be contributed to the excessive use of radical initiator, inducing a reductive cleavage of the disulfide bond by transfer reactions with the disulfide, which is described for various disulfides.[54] Thus, the molar excess of AMDVN was reduced to 15 equivalents. Due to the lower concentration of free radicals during the deactivation reaction, less interaction of radical molecules with the pyridyl disulfide side chain units was expected. In fact, after the alteration of the procedure, no loss of reactive PDSM groups could be detected within the accuracy of ^{1}H-NMR measurement.

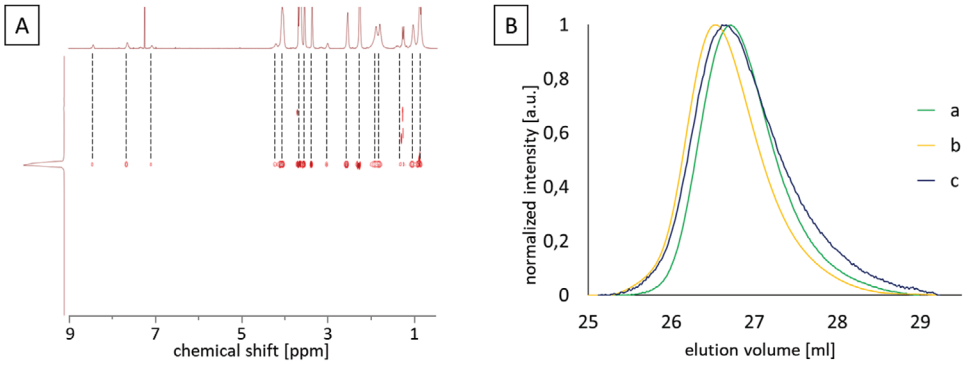

Figure 4. A) DOSY-NMR of the triblock-copolymer. B) Superimposed SEC data ((a) P1-4 homopolymer, (b) P2-4 diblock-copolymer, and (c) P3-4 triblock-copolymer).

© 2021 The Authors. Macromolecular Chemistry and Physics published by Wiley-VCH GmbH

15213935, 2021, 16, Downloaded from https://onlinelibrary.wiley.com/doi/10.1002/macp.202100122 by Cochrane Germany, Wiley Online Library on [17/10/2022]. See the Terms and Conditions (https://onlinelibrary.wiley.com/terms-and-conditions) on Wiley Online Library for rules of use; OA articles are governed by the applicable Creative Commons License

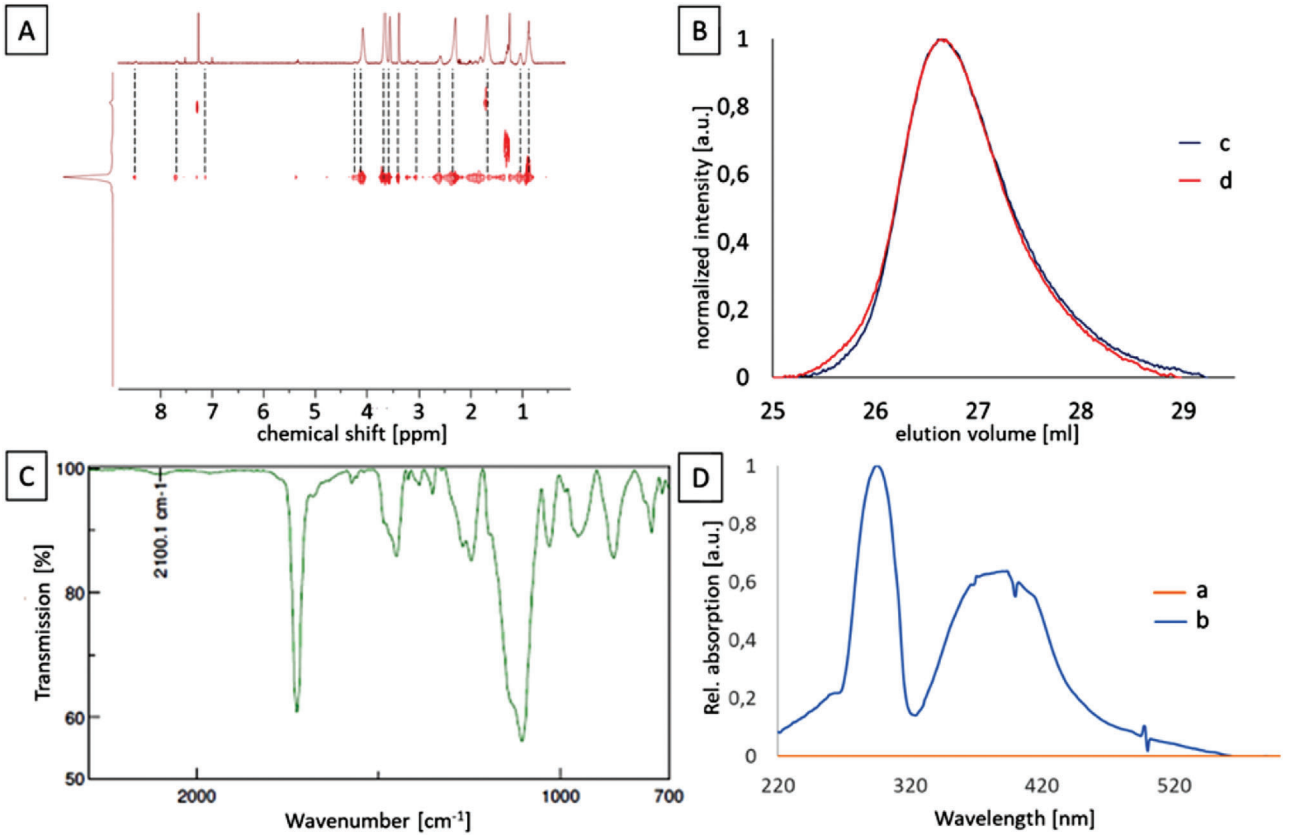

Figure 5. A) DOSY-NMR of the triblock-copolymer after deactivation of the reactive benzodithioate group. B) Superimposed SEC data of P3-4 and P4-4 with deactivated benzodithioate group. C) IR-spectrogram of P4-4. D) PDS-group reactivity test: superimposed UV–Vis data of collected centrifugate before (a) and after (b) HDT addition.

Table 4. Characterization of p(MEO_3MA)-*b*-p(PDSM)-p(DMAEMA) triblock-copolymers after deactivation of the benzodithioate group.

Polymer	DP_x [a]	DP_y [b]	DP_z [c]	M_n [d] [g mol^{-1}]	$Đ$ [e]
P4-1	30	4	25	12 520	1.24
P4-2	40	4	11	12 640	1.23
P4-3	47	10	16	16 585	1.25
P4-4	47	10	47	21 460	1.25

[a] Degree of polymerization of the MEO_3MA block; [b] Degree of polymerization of the PDSM block; [c] Degree of polymerization of the DMAEMA block; [d] Number-average molecular weight as determined by NMR spectroscopy; [e] Polydispersity as determined by SEC.

The characterization of the final triblock-copolymers, that were prepared in this way, is compiled in **Table 4**.

Altogether, it was possible to provide a shorter synthetic route for cationic triblock-copolymers with the reactive PDSM functionality as compared to the previously reported synthesis,[45] which improves the route to tailor-made and well-defined products by direct polymerization of the functional monomers.

As expected, SEC data, taken after removal of the end group, show only a minimal shift (see Figure 5B), which can be attributed to the change of the end group functionality. The monomodal course of the elugram proves that the deactivation reaction did not lead to radical cleavage of PDSM group and hence to interpolymeric disulfide exchange reactions. To test the accessibility of the PDSM side chains in post-polymerization reactions, an aliquot of P4-1 stock solution (1 mg mL^{-1} in 1,4-dioxane) was incubated with an excess of 1,6-hexanedithiol (HDT) for 10 min. This leads to a splitting of the pyridyl disulfide and to the release of 2-mercaptopyridine as side product, which is detectable in the visible light spectrum. Thereafter, the polymer was precipitated by n-hexane addition. After centrifugation, the centrifugate was analyzed using UV–Vis spectroscopy. An untreated polymer sample (a) was used as negative control. Figure 5D proves the presence of 2-mercaptopyridine in the centrifugate of the HDT treated sample (b), confirming the accessibility of PDSM side chains for modification reactions.

2.2. Self-Assembly of Polyplexes

The ability of the final triblock-copolymers (P4-1 to P4-4) to form polyplexes was tested via agarose gel electrophoresis and via dynamic light scattering (DLS). For the assembly of polyplexes pGL3-BASIC pDNA,[55] a commercially available luciferase reporter plasmid vector, was used (for further details see the Supporting Information). The vector has a length of 4818 base pairs which translates to 9636 anionic phosphate groups per pDNA.

© 2021 The Authors. Macromolecular Chemistry and Physics published by Wiley-VCH GmbH

15213935, 2021, 16, Downloaded from https://onlinelibrary.wiley.com/doi/10.1002/macp.202100122 by Cochrane Germany, Wiley Online Library on [17/10/2022]. See the Terms and Conditions (https://onlinelibrary.wiley.com/terms-and-conditions) on Wiley Online Library for rules of use; OA articles are governed by the applicable Creative Commons License

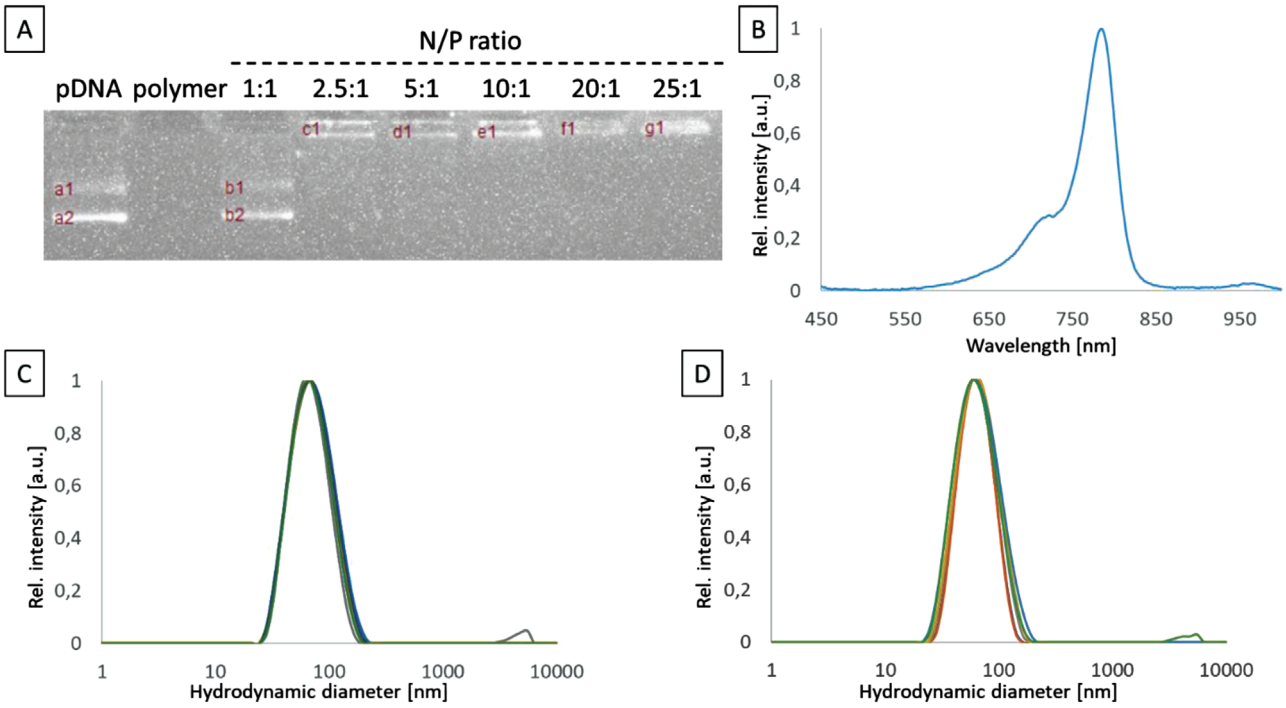

Figure 6. A) DNA retention experiment: agarose gel electrophoresis of P4-1 based polyplexes. B) P4-1 polyplex (N/P = 3) postaggregation modification: UV–vis spectrogram of 800CW DBCO-modified P4-1 polyplexes. C) DLS data ($N = 6$) of P4-1 polyplexes (N/P = 3). D) DLS data ($N = 6$) of P4-1 polyplexes (N/P = 3), crosslinked with HDT (theoretical crosslinking density: 100%).

Table 5. Results of DLS and zeta potential measurements for polyplexes prepared at an N/P-ratio of 3:1.

	Non-crosslinked polyplexes[a)]		Crosslinked polyplexes[b)]	
Polymer	Mean hydrodynamic diameter[nm]	Mean PDI	Mean hydrodynamic diameter[nm]	Mean PDI
P4-1	64.4	0.153	59.2	0.139
P4-2	97.9	0.239	103.4	0.235
P4-4	70.3	0.239	74,4	0253
Polymer	Mean ζ potential[mV]	ζ Deviation[mV]	Mean ζ potential[mV]	ζ Deviation[mV]
P4-1	+7.9	±8.8	+10.3	±14.5
P4-2	−9.4	±7.4	−12.3	±5.2
P4-4	+17.5	±12.1	+3.6	±7.2

[a)] Non-crosslinked polyplexes were prepared with an N/P-ratio of 3:1; [b)] Crosslinked polyplexes were prepared with an N/P-ratio of 3:1 and crosslinked with HDT (100% theoretical crosslinking density).

Polymer- and pDNA-stock solutions were combined by centrifugation at different amine to phospate ratios (nitrogen to phosphate ratio; N/P ratio). After merging the solutions via centrifugation and vortexing the sample for 15 s, the samples were incubated for 45 min at room temperature. For agarose gel electrophoresis, DLS- and zeta potential measurements a final pDNA concentration of 6.7×10^{-3} mg mL^{-1} was prepared.

As agarose gel electrophoresis (**Figure 6**A) shows, stable complexation of the pDNA could be achieved above N/P ratios of about 2.5:1. At lower N/P ratios, diffusion of pDNA into the gel, and therefore only incomplete or labile polyplex formation, took place. A similar onset of polyplex stability was found for all P4 polymers, which is reasonable as their block ratio does not differ strongly. To be well in the stability range, polyplexes with an N/P-ratio of 3:1 were studied for all polymers by dynamic light scattering and zeta potential measurements (see the results in Figure S6, Supporting Information). DLS measurements show, that all polymers form nanosized polyplexes with narrow size distributions (see Figure 6 and **Table 5**). Thereby, especially the polymers with a larger cationic block (P4-1 and P4-4) form small and well-defined polyplexes (60 to 70 nm diameter). Since all polyplexes were prepared at the same N/P ratio, this effect might arise from the smaller polymer content in the polyplexes at higher cationic chain lengths. The polyplexes can be stabilized by crosslinking

© 2021 The Authors. Macromolecular Chemistry and Physics published by Wiley-VCH GmbH

15213935, 2021, 16, Downloaded from https://onlinelibrary.wiley.com/doi/10.1002/macp.202100122 by Cochrane Germany, Wiley Online Library on [17/10/2022]. See the Terms and Conditions (https://onlinelibrary.wiley.com/terms-and-conditions) on Wiley Online Library for rules of use; OA articles are governed by the applicable Creative Commons License

with 1,6-hexanedithiol. However, their size did not change significantly. We have not yet characterized the effect of crosslinking in detail, but we expect similar results as described by Ritt et al.[45] for similar, but not identical, polymers with a comparable amount of pyridyl disulfide. There, it was shown that crosslinking stabilizes the inclusion of DNA.[45]

All tested polyplexes had a fairly neutral to slightly positive zeta potential (see Table 5). In this context it should be mentioned that a zeta potential between −10 and +10 mV is considered to be neutral.[56] This implies that the hydrophilic p(MEO_3MA) block of the triblock-copolymer provides an excellent shielding of the charged polyplex core from the outer medium. The nearly neutral zeta potential may inhibit unspecific interaction with blood proteins and off-target cells, but it might also decrease the transfection efficiency at target cells.

2.3. In Situ Polyplex Modification

Generally, the azide end groups of the polymers can be used to modify the polyplex even after formation, if the groups are well accessible. To test this, a polyplex sample was prepared in water, as described in the Experimental Section, and an aliquot of the reactive IR dye 800CW DBCO, which is functionalized with an alkyne for strain-promoted click reaction, was added. A 0.1 μg μL^{-1} solution of the dye in dimethyl sulfoxide (DMSO) was added, corresponding to a theoretical end-group functionalization of 10%. The sample was gently treated in an orbital mixer for 6 h to facilitate the strain-promoted azide-alkyne click reaction (SPAAC). Likewise, a polymer sample of the same concentration was treated with the dye. After excessive spin filtration UV–Vis measurements (Figure 6B) revealed the successful modification of the polyplex with the dye. At the same time, no detectable traces of the dye could be found in the filtrate. Similar results were achieved for the respective polymer-solution, which indicates a successful modification with the intended amount of the dye. This experiment implies that a sufficient number of azide functionalities are available for modification in the polymer sample and in the periphery of the assembled polyplexes. Modification with cell type specific recognition structures could drastically improve cellular uptake and transfection efficiency of the polyplexes.

3. Conclusion

This paper demonstrates that RAFT polymerization with low-temperature initiator can be used to synthesize a versatile and highly modifiable triblock-copolymer system that is applicable for the self-assembly of pDNA polyplexes.

Polymers were synthesized in three successive reactions giving a high control over the individual degrees of polymerization, leading to well-defined polymer products with narrow molecular weight distributions. After deactivation of the reactive benzothioate group with a reduced amount of radical initiator (AMDVN), the reactive disulfides (pyridyldisulfide units, PDSM) were still present in the polymers. Thus, we expect them to be rather similar to the triblock-copolymers we previously reported, which are prepared by an additional reaction on the preformed polymer.[45]

In addition to that, the triblock-copolymers were able to form stable polyplexes at low N/P ratios, starting from about N/P = 2.5. The assembled polyplexes have hydrodynamic diameters of about 60 to 100 nm and are uniform. UV–Vis spectroscopy shows, that the PDSM reactive side chain groups can be addressed by dithiol crosslinking agents, even after polyplex formation, rather similar to polyplexes described previously.[45] Furthermore, the conservation of the azide end group of the triblock-copolymer could be confirmed after the synthesis. It could be demonstrated that the azide end group of the polymer can be modified in both, the polymer and the polyplexes, utilizing a reactive DBCO 800CW IR dye by a strain promoted click reaction, which allows dye labeling and/or the labeling with binding/targeting units. This might be essential for future transfection experiments, as zeta-measurement data imply that the charged core of the polyplexes is efficiently shielded from the outer medium, which may lead to both, drastically reduced unwanted and wanted interaction with the biological environment. Incorporation of cell type specific recognition patterns could be crucial for further investigation.

The results of this paper show the potential of the triblock-copolymer system, being highly versatile and modifiable. This polymer system could be a promising candidate for a pDNA transport system that can be easily modified to meet any custom demands concerning imaging, teranostics, and codelivery of drugs, in a broad range of target cells. However, extensive studies on polyplex stability and transfection efficiency have jet to be undertaken.

4. Experimental Section

General: All chemicals and reagents that are mentioned in this paper were purchased from commercial sources and, if not stated otherwise, used without further purification. Dichloromethane was dried over calcium hydride, tetrahydrofuran, and 1,4-dioxane were dried over sodium. The dried organic solvents were freshly distilled from stock before usage. TBE buffer solution, which was used for agarose gel electrophoresis, was prepared by dissolving 10.8 g 2-amino-2-(hydroxymethyl)-1,3-propanediol (Trizma base, Sigma-Aldrich), 5.5 g boric acid (Sigma Aldrich), 0.7g 2,2′,2″,2‴-(ethane-1,2-diyldinitrilo)tetraacetic acid (Sigma-Aldrich) in 1 L of MilliQ water.

Small Molecule Synthesis: Prior to polymer synthesis the azide-bearing CTA 1-azido-25-cyano-22-oxo-3,6,9,12,15,18-hexaoxa-21-azahexadodecan-25-yl benzothioate and the monomer PDSM were synthesized in a similar manner as previously reported.[45]

General Polymer Synthesis: The sequential steps of the polymer synthesis are depicted in Scheme S1. For the synthesis of the block-copolymers that are featured in this study, the RAFT polymerization process was utilized. As mentioned above, 1-azido-25-cyano-22-oxo-3,6,9,12,15,18-hexaoxa-21-azahexadodecan-25-yl benzothioate was used as chain transfer agent and AMDVN was utilized as low temperature initiator agent. All polymerization reactions were conducted in 1,4-dioxane and a temperature of 40 °C. The monomer-conversion was determined, using ^{1}H-NMR spectroscopy. After reaching target conversion, the reaction was quenched by dipping the reaction vessel in liquid nitrogen until the reaction mixture solidified. The polymer was isolated and purified by subsequent precipitation of the solution against n-hexane and subsequent drying in vacuum at room temperature over several days.

Deactivation of the CTA End Group: The reactive CTA end group was removed by subjecting the triblock-copolymer to a 15-fold excess of AMDVN at a temperature of 40 °C. The deactivation was monitored via UV–Vis spectroscopy. After full conversion was achieved, the polymer was isolated by precipitation and dried in vacuo (as mentioned above).

© 2021 The Authors. Macromolecular Chemistry and Physics published by Wiley-VCH GmbH

15213935, 2021, 16, Downloaded from https://onlinelibrary.wiley.com/doi/10.1002/macp.202100122 by Cochrane Germany, Wiley Online Library on [17/10/2022]. See the Terms and Conditions (https://onlinelibrary.wiley.com/terms-and-conditions) on Wiley Online Library for rules of use; OA articles are governed by the applicable Creative Commons License

Polyplex Formation: For the self-assembly of pDNA polyplexes, pDNA and the triblock-copolymers were dissolved respectively in PBS buffer as stock solutions. To facilitate the polyplex formation, the amount of protonatable tertiary amine groups (N-number) per milligram polymer was calculated. Likewise, the amount of phosphate groups per milligram pDNA was determined (P-number). For different for different N/P ratios, the respective amount of the stock solutions was transferred to different spots on the inner side of a 1.5 Eppendorf vial. Depending on the experiment, PBS buffer (agarose gel electrophoresis) or 10×10^{-3} M NaCl solution (Zeta- and DLS-measurements) was added to adjust the final pDNA-concentration of 6.7×10^{-3} mg mL^{-1}. The polyplex formation was facilitated by combining the components via centrifugation at 6000 rpm for 10 s and applying additional shear force by vortexing the sample for 10 s. Afterward, samples were incubated for 45 min.

Crosslinking Polyplexes: To test the crosslinkability of the polyplexes, HDT was used as model component. After the initial incubation of the polyplexes, HDT was added according to the desired crosslinking density. After combining the solutions via centrifugation and after vortexing the sample as described above, the polyplex sample was incubated for additional 45 min at room temperature.

Agarose Gel Electrophoresis: 0.80% agarose gels were prepared, dissolving 1.20 g agarose powder in 160 mL TBE buffer solution at the boiling point of the buffer solution. For staining purpose 16 µl of 10 000× GelRed was added. After 2 h of g in a cast form, the gel was suspended in TBE buffer. Electrophoresis was conducted at 120 V and 300 mA for 30 min. The gel was analyzed on an optical bench under UV-light.

Dynamic Light Scattering and Zeta Potential Measurements: For DLS and Zeta potential measurements, a Malvern Zetasizer NanoZS, equipped with a 633 nm He/Ne laser was utilized. Data were acquired at a solution temperature of 25 °C and a fixed scattering angle of 173°. Samples were prepared in a similar fashion as described above. Aliquots of 3 µg pDNA and respective amounts of polymer stock solution, 10×10^{-3} M NaCl and crosslinking agent were used. All samples were filtered through a GHP syringe filter with a pore size of 0.4 µm prior to the measurements.

Supporting Information

Supporting Information is available from the Wiley Online Library or from the author.

Acknowledgements

The authors thank the DFG (SFB 1066, TP B05) for support.

Open access funding enabled and organized by Projekt DEAL.

Conflict of Interest

The authors declare no conflict of interest.

Data Availability Statement

Research data are not shared.

Keywords

polyplex formation with DNA, pyridyldisulfidethyl methacrylate, RAFT polymerization

Received: April 8, 2021
Revised: May 31, 2021
Published online: June 16, 2021

[1] S. C. De Smedt, J. Demeester, W. E. Hennink, *Pharm. Res.* **2000**, *17*, 113.
[2] T. Park, J. Jeong, S. Kim, *Adv. Drug Delivery Rev.* **2006**, *58*, 467.
[3] S. Y. Wong, J. M. Pelet, D. Putnam, *Prog. Polym. Sci.* **2007**, *32*, 799.
[4] M. A. Mintzer, E. E. Simanek, E. E. Simanek, *Chem. Rev.* **2009**, *109*, 259.
[5] Y. Xiang, N. N. L. Oo, J. P. Lee, Z. Li, X. J. Loh, *Drug Discovery Today* **2017**, *22*, 1318.
[6] Z. Zhou, X. Liu, D. Zhu, Y. Wang, Z. Zhang, X. Zhou, N. Qiu, X. Chen, Y. Shen, *Adv. Drug Delivery Rev.* **2017**, *115*, 115.
[7] Y. Matsumura, K. Kataoka, *Cancer Sci.* **2009**, *100*, 572.
[8] A. Kakkar, G. Traverso, O. C. Farokhzad, R. Weissleder, R. Langer, *Nat. Rev. Chem.* **2017**, *1*, 0063.
[9] T. Sun, Y. S. Zhang, B. Pang, D. C. Hyun, M. Yang, Y. Xia, *Angew. Chem., Int. Ed.* **2014**, *53*, 12320.
[10] R. Duncan, *Nat. Rev. Drug Discovery* **2003**, *2*, 347.
[11] H. Ringsdorf, *J. Polym. Sci., Polym. Symp.* **1975**, *51*, 135.
[12] D. N. Nguyen, J. J. Green, J. M. Chan, R. Langer, D. G. Anderson, *Adv. Mater.* **2009**, *21*, 847.
[13] I. Alberg, S. Kramer, M. Schinnerer, Q. Hu, C. Seidl, C. Leps, N. Drude, D. Möckel, C. Rijcken, T. Lammers, M. Diken, M. Maskos, S. Morsbach, K. Landfester, S. Tenzer, M. Barz, R. Zentel, *Small* **2020**, *16*, 1907574.
[14] C. L. Grigsby, K. W. Leong, *J. R. Soc., Interface* **2010**, *7*, 67.
[15] C. Cheng, A. J. Convertine, P. S. Stayton, J. D. Bryers, *Biomaterials* **2012**, *33*, 6868.
[16] L. Zhang, W. Liu, L. Lin, D. Chen, M. H. Stenzel, *Biomacromolecules* **2008**, *9*, 3321.
[17] Z. Jia, L. Wong, T. P. Davis, V. Bulmus, *Biomacromolecules* **2008**, *9*, 3106.
[18] T. Yildirim, A. Traeger, E. Preussger, S. Stumpf, C. Fritzsche, S. Hoeppener, S. Schubert, U. S. Schubert, *Macromolecules* **2016**, *49*, 3856.
[19] A. Ardana, A. K. Whittaker, K. J. Thurecht, *Macromol. Res.* **2017**, *25*, 599.
[20] P. Huang, J. Liu, W. Wang, C. Li, J. Zhou, X. Wang, L. Deng, D. Kong, J. Liu, A. Dong, *ACS Appl. Mater. Interfaces* **2014**, *6*, 14631.
[21] S. Agarwal, Y. Zhang, S. Maji, A. Greiner, *Mater. Today* **2012**, *15*, 388.
[22] R. J. Christie, N. Nishiyama, K. Kataoka, *Endocrinology* **2010**, *151*, 466.
[23] F. Caruso, T. Hyeon, V. M. Rotello, *Chem. Soc. Rev.* **2012**, *41*, 2537.
[24] D. Fischer, Y. Li, B. Ahlemeyer, J. Krieglstein, T. Kissel, *Biomaterials* **2003**, *24*, 1121.
[25] O. Samsonova, C. Pfeiffer, M. Hellmund, O. M. Merkel, T. Kissel, *Polymers* **2011**, *3*, 693.
[26] J. Li, J. Zhao, J. Gao, J.u Liang, W. Wu, L. Liang, *New J. Chem.* **2016**, *40*, 7222.
[27] X. Zheng, T. Zhang, X. Song, L. Zhang, C. Zhang, S. Jin, J. Xing, X.-J. Liang, *J. Mater. Chem. B* **2015**, *3*, 4027.
[28] M. Ahmed, R. Narain, *Prog. Polym. Sci.* **2013**, *38*, 767.
[29] W. T. Godbey, K. K. Wu, A. G. Mikos, *J. Controlled Release* **1999**, *60*, 149.
[30] M. Billing, T. Rudolph, E. Täuscher, R. Beckert, F. Schacher, *Polymers* **2015**, *7*, 2478.
[31] R. Hoogenboom, *Angew. Chem., Int. Ed.* **2009**, *48*, 7978.
[32] Y. Wang, H.-H. Su, Y. Yang, Y. Hu, L. U. Zhang, P. Blancafort, L. Huang, *Mol. Ther.* **2013**, *21*, 358.
[33] K. Kunath, A. Von Harpe, H. Petersen, D. Fischer, K. Voigt, T. Kissel, U. Bickel, *Pharm. Res.* **2002**, *19*, 810.
[34] E. Haladjova, M. Smolíček, I. Ugrinova, D. Momekova, P. Shestakova, Z. Kroneková, J. Kronek, S. Rangelov, *J. Appl. Polym. Sci.* **2020**, *137*, 49400.

 © 2021 The Authors. Macromolecular Chemistry and Physics published by Wiley-VCH GmbH

15213935, 2021, 16, Downloaded from https://onlinelibrary.wiley.com/doi/10.1002/macp.202100122 by Cochrane Germany, Wiley Online Library on [17/10/2022]. See the Terms and Conditions (https://onlinelibrary.wiley.com/terms-and-conditions) on Wiley Online Library for rules of use; OA articles are governed by the applicable Creative Commons License

[35] R. Laga, R. Carlisle, M. Tangney, K. Ulbrich, L. W. Seymour, *J. Controlled Release* **2012**, *161*, 537.
[36] W. Zhang, K. Müller, E. Kessel, S. Reinhard, D. He, P. M. Klein, M. Höhn, W. Rödl, S. Kempter, E. Wagner, *Adv. Healthcare Mater.* **2016**, *5*, 1493.
[37] I. Martin, C. Dohmen, C. Mas-Moruno, C. Troiber, P. Kos, D. Schaffert, U. Lächelt, M. Teixidó, M. Günther, H. Kessler, E. Giralt, E. Wagner, *Org. Biomol. Chem.* **2012**, *10*, 3258.
[38] S. Venkataraman, W. L. Ong, Z. Y. Ong, S. C. Joachim Loo, P. L. Rachel Ee, Y. Y. Yang, *Biomaterials* **2011**, *32*, 2369.
[39] K. Tappertzhofen, F. Weiser, E. Montermann, A. Reske-Kunz, M. Bros, R. Zentel, *Macromol. Biosci.* **2015**, *15*, 1159.
[40] U. Lächelt, E. Wagner, *Chem. Rev.* **2015**, *115*, 11043.
[41] P. Heller, A. Birke, D. Huesmann, B. Weber, K. Fischer, A. Reske-Kunz, M. Bros, M. Barz, *Macromol. Biosci.* **2014**, *14*, 1380.
[42] Q. Chen, K. Osada, Z. Ge, S. Uchida, T. A. Tockary, A. Dirisala, A. Matsui, K. Toh, K. M. Takeda, X. Liu, T. Nomoto, T. Ishii, M. Oba, Y. Matsumoto, K. Kataoka, *Biomaterials* **2017**, *113*, 253.
[43] Y. Cheng, R. C. Yumul, S. H. Pun, *Angew. Chem., Int. Ed.* **2016**, *55*, 12013.
[44] P. Heller, J. Zhou, B. Weber, D. Hobernik, M. Bros, F. Schmid, M. Barz, *Small* **2017**, *13*, 1603694.
[45] N. Ritt, S. Berger, E. Wagner, R. Zentel, *ACS Appl. Polym. Mater.* **2020**, *2*, 5469.
[46] E. Haladjova, V. Chrysostomou, M. Petrova, I. Ugrinova, S. Pispas, S. Rangelov, *Macromol. Biosci.* **2020**, *21*, 2000352.
[47] L. Nuhn, L. Kaps, M. Diken, D. Schuppan, R. Zentel, *Macromol. Rapid Commun.* **2016**, *37*, 924.
[48] L. Kaps, N. Leber, A. Klefenz, N. Choteschovsky, R. Zentel, L. Nuhn, D. Schuppan, *Cells* **2020**, *9*, 1905.
[49] P. Heller, D. Hobernik, U. Lächelt, M. Schinnerer, B. Weber, M. Schmidt, E. Wagner, M. Bros, M. Barz, *J. Controlled Release* **2017**, *258*, 146.
[50] T. Yildirim, A. Traeger, E. Preussger, S. Stumpf, C. Fritzsche, S. Hoeppener, S. Schubert, U. S. Schubert, *Macromolecules* **2016**, *49*, 3856.
[51] L. Sun, J. Liu, H. Zhao, *Polym. Chem.* **2014**, *5*, 6584.
[52] F. Meng, W. E. Hennink, Z. Zhong, *Biomaterials* **2009**, *30*, 2180.
[53] S. Kramer, J. Langhanki, M. Krumb, T. Opatz, M. Bros, R. Zentel, *Macromol. Biosci.* **2019**, *19*, 1800481.
[54] K. Shanmugananda Murthy, K. Ganesh, K. Kishore, *Polymer* **1996**, *37*, 5541.
[55] Promega. pGL3 Luciferase Reporter Vectors Protocol, https://www.promega.es/products/luciferase-assays/genetic-reporter-vectors-and-cell-lines/pgl3-luciferase-reporter-vectors/?catNum=E1751#resources (accessed: March 2021).
[56] M. C. Smith, R. M. Crist, J. D. Clogston, S. E. Mcneil, *Anal. Bioanal. Chem.* **2017**, *409*, 5779.

 © 2021 The Authors. Macromolecular Chemistry and Physics published by Wiley-VCH GmbH

15213935, 2021, 16, Downloaded from https://onlinelibrary.wiley.com/doi/10.1002/macp.202100122 by Cochrane Germany, Wiley Online Library on [17/10/2022]. See the Terms and Conditions (https://onlinelibrary.wiley.com/terms-and-conditions) on Wiley Online Library for rules of use; OA articles are governed by the applicable Creative Commons License